ELSEVIER

Solid State Ionics 123 (1999) 67–74

SOLID STATE IONICS

Raman study of the phase transitions sequence in pure WO_3 at high temperature and in H_xWO_3 with variable hydrogen content

E. Cazzanelli[a], C. Vinegoni[b], G. Mariotto[b,*], A. Kuzmin[c], J. Purans[c]

[a]*Istituto Nazionale per la Fisica della Materia and Dipartimento di Fisica, Università della Calabria, I-87036 Arcavacata di Rende, Cosenza, Italy*

[b]*Istituto Nazionale per la Fisica della Materia and Dipartimento di Fisica, Università di Trento, Via Sommarive, 14, I-38050 Povo, Trento, Italy*

[c]*Institute of Solid State Physics, University of Latvia, Kengaraga street 8, LV-1063 Riga, Latvia*

Received 16 March 1999; accepted 22 March 1999

Abstract

An extensive investigation of the temperature dependence of Raman spectra has been carried out on WO_3 powders from room temperature to 800°C. In particular the orthorhombic-to-tetragonal phase transition occurring at about 740°C has been studied for the first time. The Raman active mode at 710 cm^{-1} of the orthorhombic phase disappears from the spectrum at temperature below the phase transition point and the Raman activity in the tetragonal phase results very low. A comparative study of hydrogenated tungsten bronzes H_xWO_3 ($x \leq 0.23$), where the same transition sequence is driven by an increase of the proton concentration from $x = 0$ to 0.23, reveals similar behaviour of the high frequency Raman active modes, which are better resolved due to the weaker anharmonic interactions.

Keywords: Pure WO_3; Hydrogenated tungsten bronzes; Phase transition; Raman spectroscopy

PACS: 63.20. − e; 64.70.Kb; 78.30. − j; 78.30.Ly

1. Introduction

The electrochromic effect in tungsten trioxide crystals (WO_3) is associated to structural modifications, causing an evolution from lower to higher symmetry phases. The different crystal phases of the pure compound have been investigated by means of several experimental techniques [1–13], and theoretical calculations have been developed to explain the polymorphism of this compound [14]. The WO_3 crystallographic structure in all the phases is composed of corner-sharing [WO_6] octahedra having different degree of distortion. The interplay between the lattice phonons and the electronic structure of WO_3 results in the occurrence of different phases, starting from the low symmetry triclinic or monoclinic phases up to the tetragonal phase. A true cubic WO_3 structure is not stable for the pure compound at any temperature below the melting point, because of a second order Jahn–Teller effect [15]. However, the amount of the lattice deformation with respect to an idealised cubic ReO_3-type phase is low enough to

*Corresponding author. Tel.: +39-0461-881-501; fax: +39-0461-881-696.

E-mail address: mariotto@alpha.science.unitn.it (G. Mariotto)

0167-2738/99/$ – see front matter
PII: S0167-2738(99)00101-0

allow for a description of the successive phase transitions in terms of condensation of the normal modes of the ideal cubic structure [16].

Previous investigations of tungsten trioxide give the following sequence of crystal structures above room temperature (RT): triclinic P $\bar{1}$ (C_i^1), from -25 to 20–30°C [1,7,9,11,12]; monoclinic (I) $P2_1/n$ (C_{2h}^5), from 20–30 to 330°C [1–3,9]; orthorhombic P*mnb* (D_{2h}^{16}), from 330 to 740°C [6]; tetragonal P4/*nmm* (D_{4h}^7), from 740°C [10] to the melting temperature (1473°C).

While the polymorphism of WO_3 at RT and below is remarkably affected by factors like the preparation route, the crystal size and the previous history, high temperature phases, on the contrary, show a good reproducibility of the results, lower hysteresis effects and independence of the phase sequence from impurity or mechanical treatments Besides, the phase transition of WO_3 into the tetragonal symmetry can be comparatively studied at RT following structural changes upon hydrogen insertion via chemical or electrochemical methods. Hydrogen intercalation modifies the electronic structure of the host WO_3 matrix, but at the same time, does not perturb very much its atomic structure: in the resulting compound H_xWO_3, labeled as hydrogen tungsten bronze, small hydrogen ions are distributed among interstitial sites of the host crystal and are weakly bound to the host structure allowing for the high ionic mobility. The phase sequence in H_xWO_3 compounds is the following: monoclinic (I) for $0 < x < 0.1$, orthorhombic for $0.1 < x < 0.15$, tetragonal B for $0.15 < x < 0.23$, tetragonal A for $0.23 < x < 0.5$ and cubic for $x > 0.5$ [17,18].

The vibrational spectroscopy can provide very useful information on the phase transitions in tungsten oxide, complementary to that obtained by diffraction techniques. Until now, Raman and IR spectroscopic studies have been widely used for the phases close to room temperature (RT) [19,20] but, to our knowledge, no data has been reported for the orthorhombic-to-tetragonal phase transition, occurring at 740°C in the pure oxide, and no Raman study is reported on crystalline hydrogenated tungsten bronzes.

In this paper, we report on the comparative Raman spectroscopy study of the phase sequence monoclinic-orthorhombic-tetragonal, occurring in pure-WO_3 powder at high temperatures and in hydrogen bronzes (H_xWO_3) with different hydrogen contents.

2. Experimental

2.1. Sample preparation

The starting material for the present study is commercial stoichiometric WO_3 powder ('Reahim', Russia) for optical industrial applications, with a nominal purity of 99.998% ($V < 5 \times 10^{-4}$%, $Fe < 5 \times 10^{-4}$%, $Co < 1 \times 10^{-4}$%, $Mn < 1 \times 10^{-4}$%, $Cu < 1 \times 10^{-4}$%, $Ni < 1 \times 10^{-4}$%, $Cr < 5 \times 10^{-4}$%) and a pale yellow colour. The stoichiometry of the powder WO_3 (at least 2.999) was controlled by EPR measurements down to helium temperature and no EPR signals of impurity or defects were found. Preliminary spectroscopic measurements, performed with different excitation laser lines indicate no luminescence in the visible wavelengths, and no vibrational bands assignable to surface water or OH groups. Before the spectroscopic investigations this powder had a long storage time (order of years) in equilibrium with atmospheric oxygen, so that any reduction process occurred during its preparation was reversed. In fact, other experiments on purposely reduced powder samples, via milling or other treatments, showed that long interaction with air at RT induced full reoxidation of the powders [21,22]. An inspection by the optical microscope indicates that these powders have an average grain size of the order of the μm.

Hydrogenated samples with a general composition H_xWO_3 were obtained by H^+ insertion into the virgin WO_3 powder placed in 1 N aqueous solution of sulphuric acid in the presence of indium as catalyst. The hydrogen content was estimated by comparison of X-ray powder diffraction patterns for our samples with that available in the literature. The as prepared samples had deep-blue colour and the composition with $x \approx 0.23$ [23] showed the tetragonal phase structure (JCPDF-ICDD 20-483). Upon hydrogen loss, they transformed first into orthorhombic H_xWO_3 with $x \approx 0.1$ phase (JCPDF-ICDD 6-210) and later turned into monoclinic (I) WO_3.

2.2. Experimental apparatus

Pure and hydrogenated tungsten oxide samples were analyzed by powder X-ray diffraction (XRD) and Raman spectroscopy.

The samples for XRD were prepared by deposition on a Millipore filter of the powder from an aqueous suspension driven by a vacuum pump. The X-ray diffractometer was a model Bragg–Brentano, made by ItalStructures, working with the Cu Kα radiation. The X-ray diffractograms were recorded at RT in the angle range $2\theta = 20–65°$ and a step $\Delta(2\theta) = 0.05°$.

The Raman measurements have been performed by using a 1 meter focal length double monochromator Jobin–Yvon (Ramanor, model HG2-S) equipped with holographic gratings (2000 grooves/mm). The spectra were excited by the 530.9 nm line of a Krypton laser, which was operated so that the power entering in the microscope was maintained below 10 mW. The spectral resolution was of the order of 3 cm^{-1}. The scattered radiation was detected by a cooled (−35°C) photomultiplier tube (RCA, model C31034A-02), operated in photon counting mode. The signal was stored into a multichannel analyzer and then sent to a microcomputer for the analysis. For the temperature dependence study, the experimental arrangement was set in the standard macro-Raman configuration, with a right angle scattering geometry.

Measurements in the high temperature range (up to 800°C) have been made by inserting the powder samples into a fused quartz cuvette with flat walls (made by Helios Italquartz) within an optical oven, which allowed a temperature stability of about ±1°C. All the heating process occurred in air and the cuvette arrangement and closure allowed for an exchange of oxygen between powder samples and air. These conditions are not favourable to reduction reactions, usually detectable via the change from pale yellow to bluish colour. Again, other powder samples, previously reduced via mechanical treatments, underwent a total reoxidation after high temperature annealing in air, as demonstrated by the colour turning back to yellow [21,22], even more effective than the reoxidation obtained after long time exposure to air at RT. In addition heating above 300°C strongly reduced the defect disorder in such samples and favoured the transition of the powders to ordered monoclinic (I) phase [21,22].

3. Results and discussion

3.1. Normal modes analysis

The low symmetry crystal structures of WO_3 exhibit many vibrational bands, due to the high number of atoms per unit cell and to the removal of any degeneracy of the modes. However, the number of the observed peaks can be lower than that of the expected ones. This disagreements occurs when the splitting between different modes is smaller than the experimental bandwidths, or else when the Raman tensor elements associated to some mode, in principle non-zero on the basis of group theoretical considerations, are very small. At increasing temperatures both the cases become more probable, because of the strong anharmonic broadening.

With regard to the crystal phases concerned in the present investigation, in order of increasing temperatures, the standard group theory analysis gives these expected numbers for the Raman modes:

(i) In the monoclinic (I) phase, space group $P2_1/n$ (C_{2h}^5), each unit cell contains eight formula units [9] and the total representation corresponds to 96 normal modes; among these 48 are Raman active.

$$\Gamma(\text{Raman}) = 24\,A_g + 24B_g$$

The A_g modes have a Raman tensor with non-zero diagonal element and the *xz* components (labeling as *y* the unique axis). The tensor for the B_g modes contains non-zero *xy* and *yz* components.

In the previous investigation of Gabrusenok [24], on single crystal samples, 37 Raman peaks are reported, while in a previous work on the same powders analyzed here, 27 significant Raman peaks are observed at room temperature [25].

(ii) In the orthorhombic P*mnb* (D_{2h}^{16}) crystal structure, the number of formula units per unit cell is still eight [6] but the Raman representation contains a lower number of vibrational modes:

$$\Gamma(\text{Raman}) = 12A_g + 6B_{1g} + 12B_{2g} + 6B_{3g}$$

Here the Raman tensor for A_g modes contains only diagonal components, B_{1g} and B_{3g} modes have *xy* and *yz* components and B_{2g} modes have *xz* components (using the same setting of axes as above). The latter become A_g modes in the lower symmetry monoclinic phase.

A progressive decrease of the apparent band intensity is probable at increasing temperature for this crystal phase.

(iii) For the tetragonal P4/*nmm* (D^7_{4h}), containing two formula units per unit cell, the Raman representation is:

$$\Gamma(\text{Raman}) = 2A_{1g} + 2E_g$$

Thus there exists a much lower number of bands with respect to the orthorhombic phase. In addition, because the existence range of this phase is even at higher temperature, an increasing difficulty of observing all the predicted mode is expected.

3.2. Pure WO_3 at high temperatures

The Evolution of Raman spectra for pure WO_3 in the temperature range from 13 to 475°C is shown in Fig. 1. The general broadening of the bands, well visible for increasing temperatures, and the peculiar behaviour of some bands give clear indication of the monoclinic-to-orthorhombic transition.

The low frequency modes experience different shifts which can be schematised as the collapse of two vibrational modes of the monoclinic (I) phase at 34 and 60 cm^{-1} (RT values) into one of the orthorhombic phase at ~40 cm^{-1}. The intersection of the two frequencies occurs at ~300°C, corresponding to the reported monoclinic-to-orthorhombic transition point [6,16]. The two modes have the same A_g symmetry in the monoclinic phase [24], while the mode surviving in the orthorhombic phase has a B_{2g} symmetry, correspondent to A_g in the specific correlation diagram of this phase transition [19]. This evolution has been previously observed by Gabrusenoks [16,19] on single crystals, and the similar behaviour in the powder samples studied here confirms the good reproducibility of the phase transition and the connected vibrational effects for temperatures above about 300 K. It is also noteworthy to observe an interesting evolution of the relative

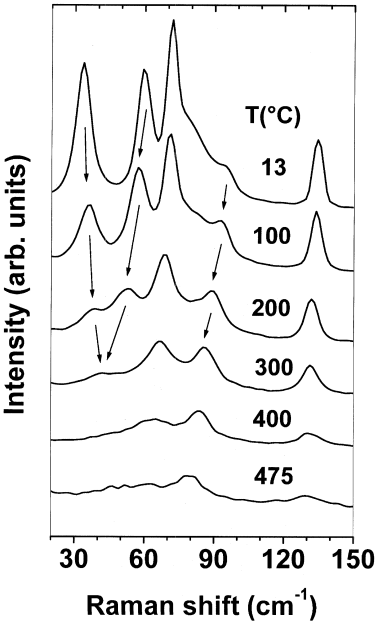

Fig. 1. Temperature dependence of the low frequency Raman modes for the tungsten trioxide WO_3 powder across the monoclinic-to-orthorhombic phase transition.

intensities of the mode at 93 cm^{-1} (*RT* value) with respect to the other low frequency vibrations. This mode, assigned to an A_g symmetry [24], appears as a shoulder of stronger bands in the monoclinic phase, whereas it becomes the dominant band at the low frequencies in the orthorhombic phase above 400°C (Fig. 1). At higher temperatures, the mode remains the only survivor among the low frequency Raman active vibrations. The precise mechanism of this intensity change is beyond the purpose of the present work, because a theoretical study of the temperature dependence for the modes approaching the transition requires a detailed knowledge of all the interatomic distances and angles, while the XRD powder measurements are mainly sensitive to the W positions, less affected by the phase-transitions. However it is reasonable to assign such low frequency vibration to the tilting motion of the oxygen cages around the tungsten atoms or to translational vibrations of different octahedral units within the same unit cell, whose polarizability modulation becomes relatively more and more strong as the lattice parameters evolve with increasing *T*.

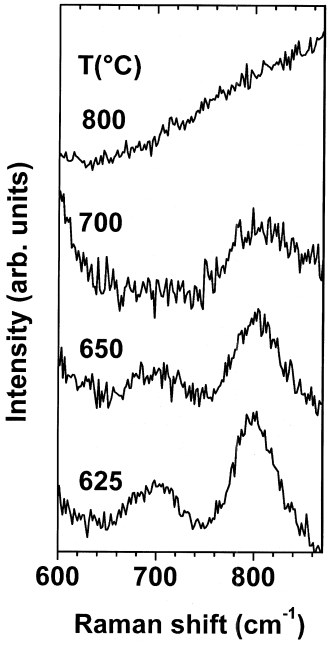

Fig. 2. Temperature dependence of the high frequency Raman modes for the tungsten trioxide WO_3 powder across the orthorhombic-to-tetragonal phase transition.

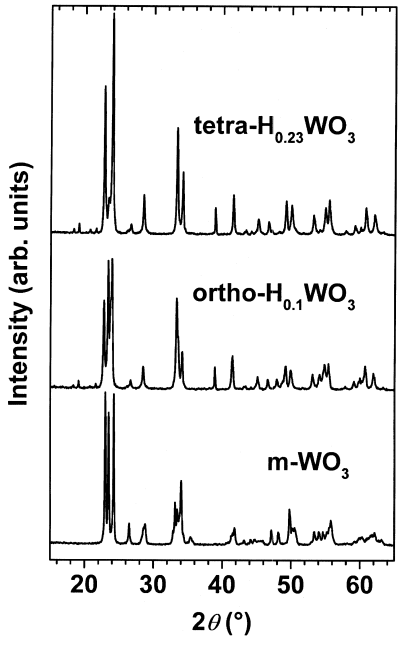

Fig. 3. XRD patterns of tetragonal and orthorhombic hydrogen tungsten bronzes H_xWO_3 and of pure monoclinic (I) tungsten trioxide WO_3.

Unfortunately, the spurious contribution of the quartz cuvette does not allow us to follow the further evolution of the frequency region below 400 cm^{-1} at temperatures higher than 500°C. Therefore, the orthorhombic-to-tetragonal phase transition was investigated through the Raman spectra only in the high frequency stretching modes (Fig. 2). It is interesting that both stretching modes at 700 and 800 cm^{-1} are no more detectable at 800°C: the lower frequency mode at 700 cm^{-1} disappears already at temperatures below the transition point (740°C [10]), while the 800 cm^{-1} mode disappears in the tetragonal phase. The monotonically increasing contribution observed at 800°C in Fig. 2 is due probably to blackbody radiation of the oven cavity or to luminescence contributions arising from the change of optical properties across the orthorhombic–tetragonal phase transition [26]. Some Raman active mode are expected to survive in the tetragonal phase [16], but the anharmonic interactions, strongly enhanced by the high temperature, surely induce a dramatic broadening of the surviving Raman bands, and this fact, together with the spurious contributions, does not allow for the detection of the 800 cm^{-1} stretching mode at $T \geq 800$°C (Fig. 2).

To check the real evolution of the Raman bands across the orthorhombic-to-tetragonal phase transition it is quite useful to study the same transition at lower temperatures. The protonated H_xWO_3 compounds, where the structural transitions are driven by the hydrogen content instead of the thermal motion, constitute a very suitable system for such study.

3.3. Hydrogenated H_xWO_3 at room temperature

The tungsten trioxide WO_3 powder transforms upon hydrogen insertion into deep-blue coloured hydrogen bronze H_xWO_3, being in the tetragonal phase for the hydrogen content $0.15 < x < 0.50$ [17,18]. However, this tungsten bronze is unstable in the ambient oxidizing atmosphere so that at increasing air exposition times after hydrogenation, the powder returns back to yellow monoclinic (I) WO_3 phase, passing through the orthorhombic H_xWO_3 ($0.1 < x < 0.15$) [17,18]. The various steps of this spontaneous evolution can be monitored by in-situ XRD experiments as shown in Fig. 3.

The blue coloration of the bronze, appearing with

the proton insertion, is associated with the colour centres corresponding to the tungsten ions in the 5+ valence state [27,28]. It causes a strong decrease of the total Raman intensity due to optical absorption. Additionally, the structural changes associated with the variable hydrogen content induce also strong changes in the intensity ratio between the various bands. As a result, the Raman spectra (see Fig. 4) show an evolution quite similar to that observed for pure WO_3 at high temperatures. Because of the fast de-hydrogenation process accelerated by the laser light heating during the Raman measurements, no quantitative estimation of the hydrogen content was possible for intermediate compositions. However, the time sequence of the spectra in Fig. 4 corresponds to a decrease of intercalated protons for the oxidizing action of the atmosphere, resulting in pure monoclinic (I) phase after two hours of measurements.

To minimize systematic errors, the spectra were collected very rapidly, losing somewhat in the signal-to-noise ratio. Besides, the data acquisition for all spectra was started from the higher frequency side to avoid a bias in the 710 cm^{-1} mode to 816 cm^{-1} mode intensity ratio, thus depressing the lower frequency mode upon de-hydrogenation process. In fact, the 710 cm^{-1} mode decreases strongly with respect to the 816 cm^{-1} mode upon hydrogen insertion, and disappears for proton concentrations lower than the maximum attainable. The above mentioned experimental procedure insures that such effect is true. This behaviour corresponds well to the observed quenching of the same mode in a temperature range below the orthorhombic-to-tetragonal transition in the case of temperature driven evolution in pure WO_3 (Fig. 2). Note that the 816 cm^{-1} stretching mode remains observable even for the highest proton content corresponding to the tetragonal $H_{0.23}WO_3$ phase. The difference between Raman spectra of pure WO_3 and H_xWO_3 bronze in tetragonal phase suggests that the missing observation of the 816 cm^{-1} stretching mode for pure WO_3 is probably due to strong anharmonic interactions present at high temperatures, beside the spurious effect of blackbody emission, contributing to increase the noise.

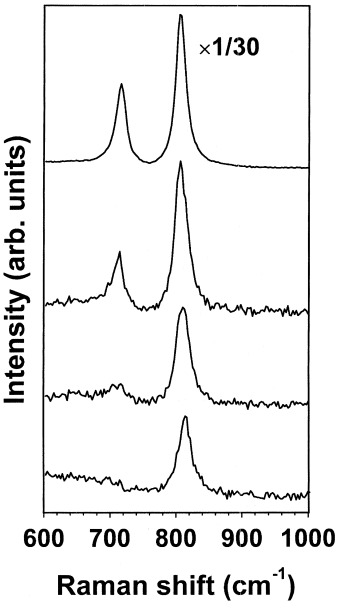

Fig. 4. Evolution of the Raman spectra for H_xWO_3 upon oxidation in air. The starting H_xWO_3 powder with the maximum hydrogen content $x=0.23$ is shown at the bottom. The top spectrum, reduced by a factor 30 to be comparable, was obtained after two hours of exposition in air and corresponds to pure monoclinic (I) WO_3. The intermediate spectra correspond to hydrogen contents in the range $0<x<0.23$.

A reasonable explanation of the existence of only one stretching mode in the tetragonal phase [10] is the symmetrization of the W–O bonds in the a–b plane, while the bonds along the c axis remains different and Raman active. In fact, the Raman spectrum of hydrogenated tungsten oxide (Fig. 5) shows a number (4) of Raman active modes lower with respect to the orthorhombic phase, but in agreement with the predictions of the group theory for the tetragonal phase.

Another interesting aspect of the Raman spectra evolution in H_xWO_3 is a dependence of the highest stretching mode frequency on hydrogen content (Fig. 4): upon de-hydrogenation, its frequency decreases from 816 cm^{-1} in $H_{0.23}WO_3$ to 806 cm^{-1} in monoclinic (I) WO_3. It is known [20] that the force constant (and thus the stretching frequency ν(W–O)) and the length of the W–O bond are strongly correlated. In Fig. 6, we used the experimental values of ν(W–O) for monoclinic (I) WO_3 from the present work and for $WO_3 \cdot H_2O$ from [20] and the values of the interatomic distances R(W–O) from [3,29]. Note that the correlation shown in Fig. 6 by solid line and the one obtained in [20] are similar and both are deduced for the six-fold coordinated

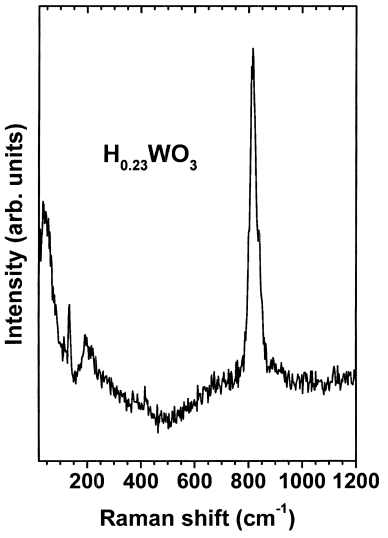

Fig. 5. Raman spectrum of tetragonal $H_{0.23}WO_3$ measured at room temperature. Only one W–O stretching mode at 816 cm^{-1} is visible in high frequency region.

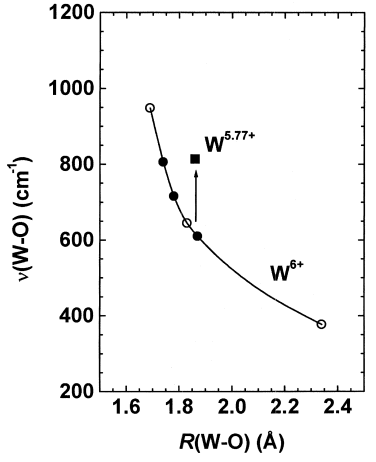

Fig. 6. Correlation between the stretching frequency ν(W–O), probed by Raman spectroscopy, and the interatomic distance R(W–O). (Note that similar correlation was obtained in [20].) Full circles correspond to experimental data for monoclinic (I) $W^{6+}O_3$ and open circles to $W^{6+}O_3 \cdot H_2O$. Square corresponds to the stretching mode in $H_{0.23}W^{5.77+}O_3$ (Figs. 4 and 5). The solid line is a guide for eyes.

tungsten ions having the valence state 6+. It is known that insertion of hydrogen into WO_3 leads to the changes in crystallographic structure and the valency of tungsten ions: a symmetrization of the tungsten local environment occurs and its valence reduces. In particular, the tungsten ions are located at the centre of octahedra formed by six oxygen atoms (four in a–b plane at 1.86 Å and two along the c-axis at 1.94 Å) in tetragonal $H_{0.23}WO_3$ [23].

Thus, one can expect from the increase of the W–O bond length that a strong decrease of the highest stretching W–O frequency should occurs in $H_{0.23}WO_3$ compared to WO_3: however, this contradicts to the experimental results shown in Fig. 4: in $H_{0.23}WO_3$, having longer W–O interatomic distances than monoclinic (I) WO_3, the frequency of the highest stretching mode does not decrease. The observed discrepancy can be attributed to the change of the valence state of tungsten ion. The dependence in Fig. 6 was obtained for compounds including only W^{6+} ions, whereas upon hydrogen bronze formation the tungsten valence state is reduced and becomes equal to 5.77+ in $H_{0.23}WO_3$. The change in the electronic structure modifies the strength of the W–O interaction and thus a different stretching frequency should be expected for the same distance. Since the reduced tungsten ions are the colour centres with polaronic absorption mechanism [26,30], the donated electron is localized at the tungsten ion sites increasing the covalence of the tungsten–oxygen bonds. As a net result, the W–O stretching frequency remarkably increases as shown in Fig. 6 by the arrow.

4. Conclusions

An extensive investigation of the temperature dependence of Raman spectra has been carried out on WO_3 powders from room temperature to 800°C. In particular, the monoclinic-to-orthorhombic and orthorhombic-to-tetragonal phase transitions were studied. The normal mode at 710 cm^{-1} disappears in the spectrum at temperature below the phase transition point and the Raman activity in the tetragonal phase results very weak.

A comparative study of hydrogenated tungsten bronzes H_xWO_3 ($x \leq 0.23$), where analogous series of transitions is driven at room temperature by an increase of the proton concentration from $x=0$ to 0.23, reveals similar behaviour of the Raman active modes. However, in H_xWO_3 compounds the Raman bands are better resolved due to the occurrence of weaker anharmonic interactions. The correlation

between the values of W–O stretching frequencies and of interatomic distances suggests a strong dependence of W–O stretching energy on the valence state of tungsten ions.

Acknowledgements

A.K. wish to thank the Centro CNR-ITC di Fisica degli Stati Aggregati ed Impianto Ionico (Trento) and the Università di Trento for hospitality and financial support.

References

[1] S. Tanisaki, J. Phys. Soc. Japan 15 (1960) 566.
[2] B.O. Loopstra, P. Boldrini, Acta Crystallogr. B 21 (1966) 158.
[3] B.O. Loopstra, H.M. Rietveld, Acta Crystallogr. B 25 (1969) 1420.
[4] E.K.H. Salje, K. Viswanathan, Acta Crystallogr. A 31 (1975) 356.
[5] E.K.H. Salje, Acta Crystallogr. A 31 (1975) 360.
[6] B. Salje, Acta Crystallogr. B 33 (1975) 574.
[7] R. Diehl, G. Brandt, E.K.H. Salje, Acta Crystallogr. B 34 (1978) 1105.
[8] T. Hirose, J. Phys. Soc. Japan 49 (1980) 562.
[9] P.W. Woodward, A. W. Sleight and T. Vogt, J Phys, Chem. Solids 56 (1995) 1305.
[10] K.L. Kehl, R.G. Hay, D. Wahl, J. Appl. Phys. 23 (1952) 212.
[11] E.K.H. Salje, S. Rehmann, F. Pobell, D. Morris, K.S. Knight, T. Herrmannsdörfer, M.T. Dove, J. Phys.: Condens. Matter 9 (1997) 6563.
[12] E.K.H. Salje, Ferroelectrics 12 (1976) 215.
[13] B. Iguchi, H. Sugimoto, A. Tamenori, H. Miyagi, J. Solid State Chem. 91 (1991) 286.
[14] J.B. Goodenough, Prog. Solid State Chem. 5 (1971) 145.
[15] M. Kawaminami, T. Hirose, J. Phys. Soc. Japan 46 (1979) 864.
[16] E.V. Gabrusenok, Lattice Dynamics of Tungsten Trioxide, in: Electrochromism. Reports of Latvian University, Latvian University, Riga, Latvia, 1987, pp. 100–110.
[17] P.G. Dickens, J.H. Moore, D.J. Neild, J. Solid State Chem. 7 (1973) 241.
[18] C. Genin, A. Driouiche, B. Gerand, M. Figlarz, Solid State Ionics 53–56 (1992) 315.
[19] E.V. Gabrusenok, Sov. Phys. Solid State 26 (1984) 2226.
[20] M.F. Daniel, B. Desbat, J.C. Lessegues, B. Gerand, M. Figlarz, J. Solid State Chem. 67 (1987) 235.
[21] E. Cazzanelli, G. Mariotto, C. Vinegoni, A. Kuzmin, J. Purans, in: K.-C. Ho, C.B. Greenberg, D.M. MacArthur (Eds.), Electrochromic Materials III, Electrochemical Society Proceedings, Vol. 96-24, The Electrochemical Society, Pennington, NJ, 1996, pp. 260–274
[22] A. Kuzmin, J. Purans, E. Cazzanelli, C. Vinegoni, G. Mariotto, J. Appl. Phys. 84 (1998) 5515.
[23] P.G. Dickens, R.J. Hurditch, Nature 251 (1967) 1266.
[24] E.V. Gabrusenok, Fizikas un technisko zinatnu serf/a 6 (1982) 67.
[25] E. Cazzanelli, G. Mariotto, C. Vinegoni, A. Kuzmin, J. Purans, J. Solid State Chem. 143 (1999) 24.
[26] E.K.H. Salje, J. Appl. Cryst. 7 (1974) 615.
[27] B.W. Faughnan, R.S. Crandal, P.M. Heyman, RCA Rev. 36 (1975) 177.
[28] O.F. Schirmer, V. Wittwer, G. Baur, J. Electrochem. Soc. 124 (1977) 749.
[29] J.T. Szymanski, A.C. Roberts, Can. Mineral. 22 (1984) 681.
[30] A. Kuzmin, J. Purans, J. Phys.: Condens. Matter 5 (1993) 2333.